Organic Electronics 17 (2015) 355–363

Contents lists available at ScienceDirect

Organic Electronics

journal homepage: www.elsevier.com/locate/orgel

Synthesis and photovoltaic properties of new small molecules with rhodanine derivative as the end-capped blocks

Yuanhang Zhou [a,d], Manjun Xiao [b], Deyu Liu [a], Zhengkun Du [a], Weichao Chen [a], Dan Ouyang [a], Liangliang Han [a], Xiaobo Wan [a], Renqiang Yang [a,c,*]

[a] CAS Key Laboratory of Bio-based Materials, Qingdao Institute of Bioenergy and Bioprocess Technology, Chinese Academy of Sciences, Qingdao 266101, China
[b] College of Chemistry, Key Lab of Environment-Friendly Chemistry and Application of the Ministry of Education, Xiangtan University, Xiangtan 411105, China
[c] State Key Laboratory of Luminescent Materials and Devices, South China University of Technology, Guangzhou 510641, China
[d] University of Chinese Academy of Sciences, Beijing 100049, China

ARTICLE INFO

Article history:
Received 30 September 2014
Received in revised form 2 December 2014
Accepted 28 December 2014
Available online 3 January 2015

Keywords:
Organic solar cells
Bulk hetero-junction
Conjugated small molecules
Electron donor
Rhodanine derivative

ABSTRACT

Two new acceptor–donor–acceptor (A–D–A) type small molecules DCAO3TIDT and DCNR3TIDT, with 4,4,9,9-tetrakis(4-(dodecyloxy)phenyl)-4,9-dihydro-s-indaceno-[1,2-b:5,6-b′]dithiophene (IDT) as the core group and 2-ethylhexyl cyanoacetate (CAO) and 2-(1,1-dicyanomethylene)-3-octyl rhodanine (CNR) as different end-capped blocks, have been designed and synthesized. Both of them have been employed as donor for solution-processed bulk hetero-junction (BHJ) organic solar cells (OSCs). The two compounds showed deep highest occupied molecular orbital (HOMO) energy levels (~−5.30 eV) and strong absorption. The DCAO3TIDT and DCNR3TIDT with $PC_{71}BM$ as acceptor based BHJ solar cell devices showed short circuit current density (J_{sc}) of 6.93 mA/cm^2 and 8.59 mA/cm^2, power conversion efficiency (PCE) of 3.34% and 4.27%, respectively, and with almost same open-circuit voltage (~0.93 V), under the illumination of AM 1.5 G, 100 mW/cm^2. The high J_{sc} for DCNR3TIDT could result from its wider and red-shifted absorption than that of DCAO3TIDT, which was probably induced by the end-capped block rhodanine derivative. The results demonstrate that the end group would be taken into full account when designing new solution-processed small molecules, which is an important factor to determine their photovoltaic properties.

1. Introduction

In recent years, bulk hetero-junction (BHJ) organic solar cells (OSCs) have made significant progress due to the attractive advantages, such as light weight, potential to low cost, and flexible [1]. Power conversion efficiency (PCE) which is higher than 9% has been reached recently [2–14]. Currently, BHJ OSCs are based on two types of donor materials, conjugated polymers and small molecules [15,16]. Compared to their conjugated polymer counterparts, small molecules offer potential advantages in terms of defined molecular structure, uniform molecular weight, easy purification, and no batch to batch variations [17–21]. Thus, solution-processed small molecules BHJ OSCs have stimulated more and more attention, and the PCE of the devices based on small molecules as the donors and fullerene derivatives as the acceptors has been up to 8% [22]. The immense progress of OSCs is mainly ascribed to the versatile chemical structures of donor–acceptor (D–A) type, which allows the molecular orbital to be easily tuned so as to emerge intra-molecular charge transfer (ICT), and

* Corresponding author at: CAS Key Laboratory of Bio-based Materials, Qingdao Institute of Bioenergy and Bioprocess Technology, Chinese Academy of Sciences, Qingdao 266101, China.
E-mail address: yangrq@qibebt.ac.cn (R. Yang).

http://dx.doi.org/10.1016/j.orgel.2014.12.031
1566-1199/

the ICT exhibits absorption band at longer wavelength direction [23,24]. Until now, a lot of efficient D building blocks have been reported, such as benzodithiophene (BDT), fluorene, dithienosilole (DTS), and indacenodithiophene (IDT). However, compared with the research of the D units, the A moieties have attracted relatively lower attention [25].

2-(1,1-Dicyanomethylene)-3-octyl rhodanine (CNR) is a new strong electron acceptor, which is rhodanine's derivative. Rhodanine is a common dye, and its derivatives have been used as acceptor moiety in a variety of push–pull organic compounds for non-linear optics, electrically conducting materials, molecular rectification, dyes, solvatochromism [26–28], and more recently, they have been used in the BHJ OSCs [22,29,30]. For improving the light absorption of the compound, malononitrile unit has been introduced into the rhodanine structure. Here CNR can bring wide absorption because both of the malononitrile and rhodanine units can guarantee strong electron accepting ability. On the other hand, 2-ethylhexyl cyanoacetate (CAO) has been proved that it is an efficient electron acceptor group, where cyano moiety and 2-ethylhexyl chain can simultaneously induce ICT band and improve solubility [31]. Thus, CAO has been chosen to compare with CNR. Among various electron donor groups, 4,4,9,9-tetrakis(4-(dodecyloxy)phenyl)-4,9-dihydro-s-indaceno[1,2-b:5,6-b′]-dithiophene (IDT) has drawn much attention because of their good photovoltaic performance [32]. The IDT can enhance inter-chain interaction of the molecules and lead to higher carrier mobility [32–36]. Herein, two acceptor–donor–acceptor (A–D–A) type molecules DCAO3TIDT and DCNR3TIDT (Scheme 1) with IDT as the core D unit, CAO and CNR as the A unit, and trithiophene as the linker have been designed and synthesized. To reduce the steric effect, there is no any side chain in the trithiophene unit [37,38]. As expected, the ability of electron withdrawing of CNR is stronger than CAO, and DCNR3TIDT shows a broad absorption than that of DCAO3TIDT, which could improve the short circuit current density (J_{sc}) and result in higher PCE for DCNR3TIDT-based OSC.

2. Experimental

2.1. Materials

5″-Bromo-[2,2′:5′,2″-terthiophene]-5-carbaldehyde, (4,4,9,9-tetrakis(4-(dodecyloxy)phenyl)-4,9-dihydro-s-indaceno[1,2-b:5,6-b′]dithiophene-2,7-diyl)bis(trimethylstannane) and 2-(1,1-dicyanomethylene)-3-octyl rhodanine were prepared according to the literature [22,35,36,39]. Solvents were dried by standard procedure and distilled before use. All of the other chemicals were purchased from Aladdin and used without further purification.

2.2. Measurements and instrumentation

NMR spectra were carried out on a Bruker Advance III 600 spectrometer using tetramethylsilane as an internal standard. High resolution mass spectra were recorded on a Bruker Maxis UHR TOF spectrometer under APCI mode. The thermogravimetric analysis (TGA) was carried out on a SDT Q600 Simultaneous DSC–TGA Instrument under purified nitrogen gas flow with a 10 °C/min heating rate. UV–vis absorption spectra were carried out on a Hitachi U-4100 spectrophotometer. Cyclic voltammetry was measured on a CHI660D electrochemical workstation. Surface roughness and morphology of thin film were characterized by atomic force microscopy (AFM) on an Agilent 5400.

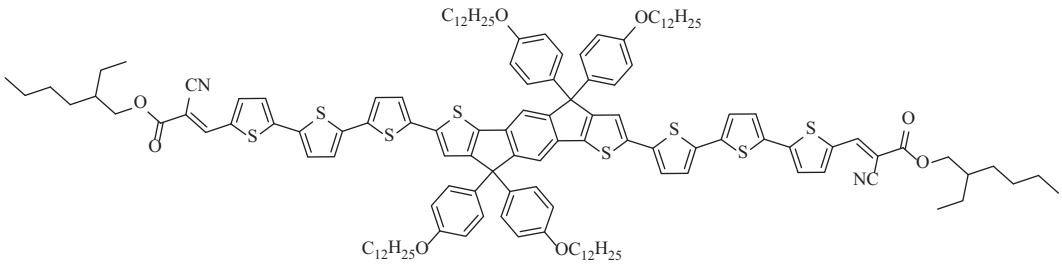

DCAO3TIDT

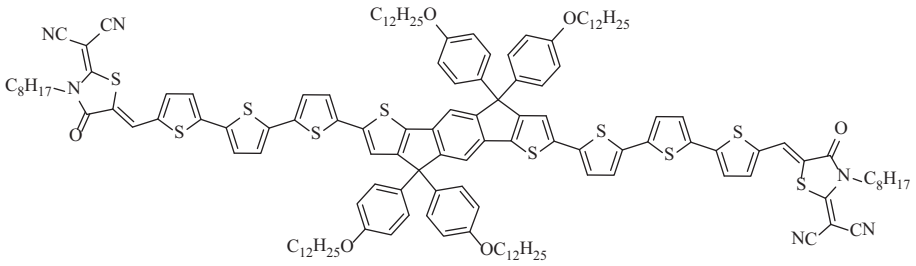

DCNR3TIDT

Scheme 1. The chemical structures of DCAO3TIDT and DCNR3TIDT.

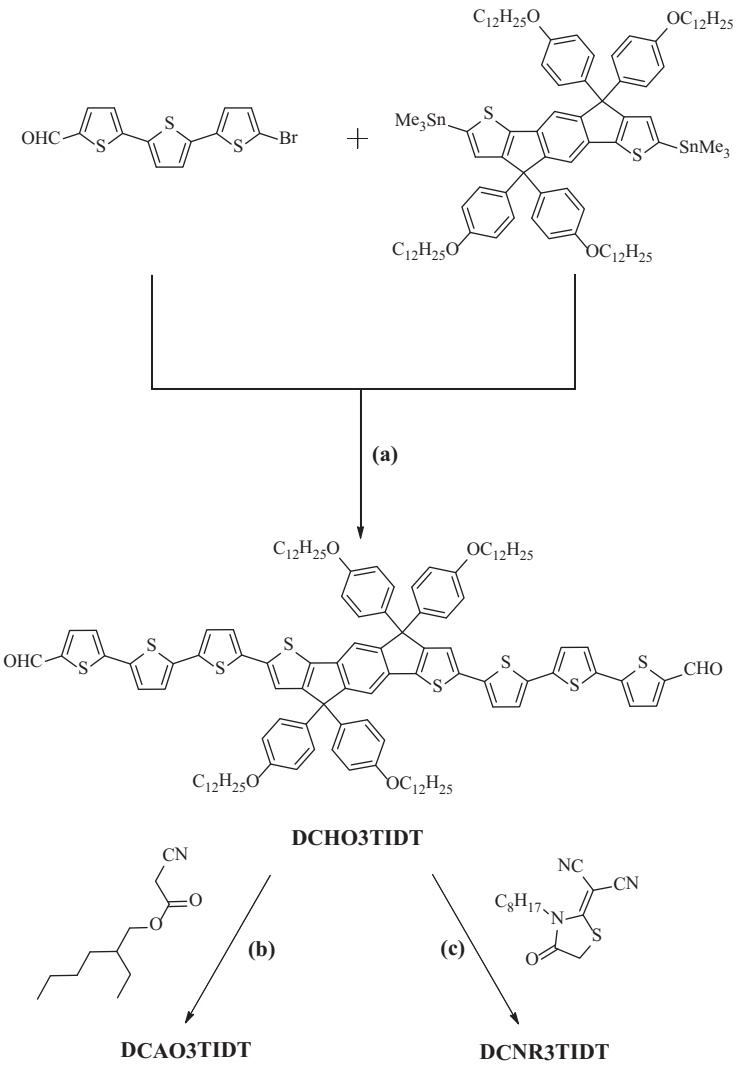

Scheme 2. Synthesis routes to the target molecules: (a) toluene, $Pd(PPh_3)_4$, argon, reflux for 48 h; (b) $CHCl_3$, triethylamine, argon, room temperature for 48 h; and (c) CH_3COOH, CH_3COONH_4, chlorobenzene, argon, reflux for 48 h.

2.3. Device fabrication and characterization of OSCs

Photovoltaic devices were fabricated by a simple spin-coating process, with a general device structure of glass/ITO/PEDOT:PSS/active layer/Ca/Al. The ITO-coated glasses were ultrasonically cleaned with acetone, toluene, methanol, and isopropyl alcohol subsequently. Oxygen plasma treatment was made for 10 min as the final step of substrate cleaning to improve the contact angle just before film coating. Onto the ITO glass a layer of polyethylenedioxythiophene–polystyrene sulfonic acid (PEDOT:PSS) film was spin-coated from its aqueous dispersion with a thickness of 40 nm. PEDOT:PSS film was dried at 160 °C for 30 min in the air. The solution of the small molecules and PCBM in $CHCl_3$ was prepared in a nitrogen-filled dry box and spin-coated on the top of the ITO/PEDOT:PSS. The typical thickness of the active layer was 100 nm. The concentration of the small molecule/PCBM blending

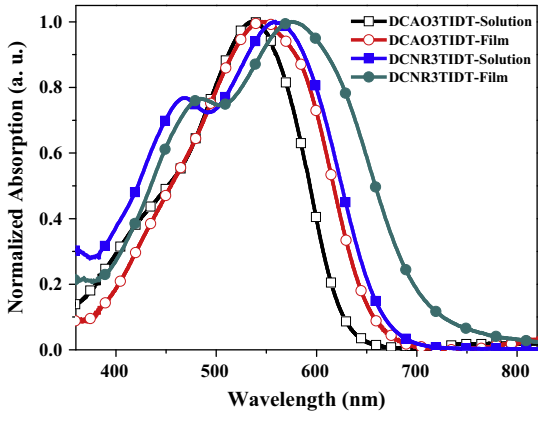

Fig. 1. UV–vis absorption spectra of DCAO3TIDT (open) and DCNR3TIDT (solid).

Table 1
Optical and electrochemical properties of DCAO3TIDT and DCNR3TIDT.

	Solution λ_{max} (nm)	Film		E_g^{opt} (eV)	φ_{ox} (V)	HOMO (eV)[a]	LUMO (eV)[b]
		λ_{max} (nm)	λ_{edge} (nm)				
DCAO3TIDT	537	546	662	1.87	0.89	−5.29	−3.42
DCNR3TIDT	468, 561	484, 576	715	1.73	0.93	−5.33	−3.60

[a] $E_{HOMO} = -e(\varphi_{ox} + 4.8 - \varphi_{1/2,\ FeCp2})$ (eV).
[b] Derived from HOMO and E_g^{opt}.

solution used in this study was 15 mg/mL. Subsequently Ca (10 nm) and Al (100 nm) were thermally deposited at a vacuum of 2×10^{-4} Pa on the top of active layer as a cathode. The current density–voltage (J–V) characteristics of the devices were measured with a Keithley 2420 source measurement unit under simulated 100 mW/cm^2 (AM 1.5 G) irradiation from a Newport solar simulator. Light intensity was calibrated with a standard silicon solar cell. The external quantum efficiencies (EQE) were analyzed using a certified Newport incident photon conversion efficiency measurement system.

2.4. Synthesis of the molecules

The synthesis routes to DCAO3TIDT and DCNR3TIDT are shown in Scheme 2. By the Knoevenagel condensation of compound DCHO3TIDT with 2-ethylhexyl cyanoacetate or 2-(1,1-dicyanomethylene)-3-octyl rhodanine, the target molecules DCAO3TIDT and DCNR3TIDT were afforded. The exact structures of the two molecules were confirmed by ^{1}H NMR spectra, ^{13}C NMR spectra and other methods.

Synthesis of DCHO3TIDT

A solution of 5″-bromo-[2,2′:5′,2″-terthiophene]-5-carbaldehyde (0.27 g, 0.76 mmol), (4,4,9,9-tetrakis(4-(dodecyloxy)phenyl)-4,9-dihydro-s-indaceno[1,2-b:5,6-b′]-dithiophene-2,7-diyl)bis(trimethylstannane) (0. 5 g, 0.31 mmol), and Pd(PPh$_3$)$_4$ (0.05 g, 0.04 mmol) in toluene (30 mL) was degassed with argon. Then the mixture was refluxed for 48 h. After the reaction was completed, the mixture was poured into water and extracted with CH_2Cl_2. The organic layer was washed with water and then dried

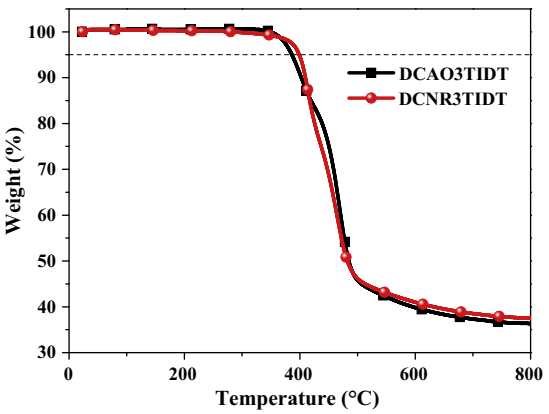

Fig. 2. TGA curves of DCAO3TIDT and DCNR3TIDT.

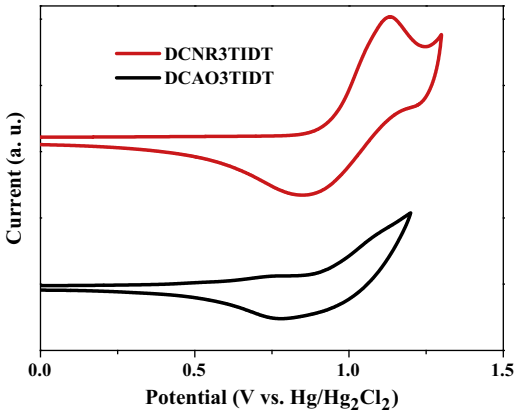

Fig. 3. Cyclic voltammograms of DCAO3TIDT and DCNR3TIDT films on glassy carbon electrode in a 0.1 mol/L n-Bu$_4$NPF$_6$ acetonitrile solution at a scan rate of 100 mV/s.

over Na_2SO_4. After removal of solvent, the crude product was purified with column chromatography on silica gel using a mixture of CH_2Cl_2 and petroleum ether (3:2) as eluant to afford compound DCHO3TIDT (0.45 g, 80%). ^{1}H NMR (600 MHz, $CDCl_3$) δ 9.85 (s, 2H), 7.66 (d, J = 3.9 Hz, 2H), 7.35 (s, 2H), 7.27 (d, J = 3.8 Hz, 2H), 7.23 (d, J = 3.9 Hz, 2H), 7.18 (d, J = 8.8 Hz, 8H), 7.11 (d, J = 3.8 Hz, 2H), 7.09 (d, J = 3.8 Hz, 2H), 7.07 (d, J = 5.1 Hz, 4H), 6.80 (d, J = 8.9 Hz, 8H), 3.91 (t, J = 6.5 Hz, 8H), 1.77–1.72 (m, 8H), 1.45–1.40 (m, 8H), 1.33–1.24 (m, 64H), 0.87 (t, J = 7.0 Hz, 12H). ^{13}C NMR (150 MHz, $CDCl_3$) δ 182.40, 158.17, 157.06, 153.78, 146.72, 141.63, 140.39, 139.33, 138.85, 138.08, 137.37, 136.14, 135.01, 134.76, 134.48, 129.02, 127.02, 125.16, 124.49, 124.06, 123.94, 119.70, 117.08, 114.31, 67.96, 62.31, 31.91, 29.66, 29.63, 29.60, 29.58, 29.40, 29.34, 29.31, 26.08, 22.69, 14.12. MS (APCI) m/z: calcd for $C_{114}H_{134}O_6S_8$ [M]$^+$, 1855.7980; found, 1855.8076.

Synthesis of DCAO3TIDT

A solution of DCHO3TIDT (0.2 g, 0.1 mmol), 2-ethylhexyl cyanoacetate (0.2 g, 1.2 mmol), and triethylamine (0.5 mL) in $CHCl_3$ (20 mL) was degassed with argon. Then the mixture was stirred for 48 h at room temperature. After the reaction was completed, the mixture was poured into water and extracted with CH_2Cl_2. The organic layer was washed with water and then dried over Na_2SO_4. After removal of solvent, the crude product was purified with column chromatography on silica gel using a mixture of CH_2Cl_2 and petroleum ether (2:1) as eluant to afford compound DCAO3TIDT (120 mg, 50%) as a black solid. ^{1}H NMR

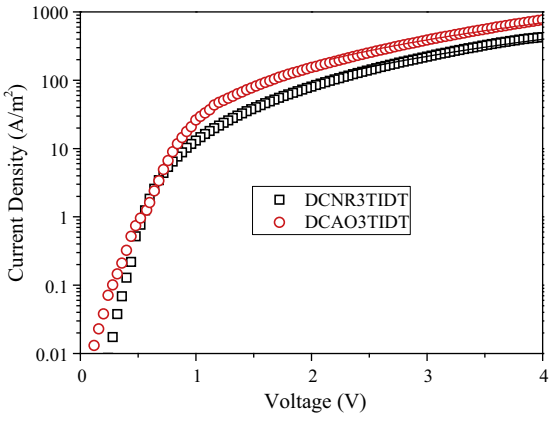

Fig. 4. The current density–voltage curves of vertical diodes. The symbols are experimental data for the transport of holes, and the solid lines are fitted according to the space-charge-limited-current model.

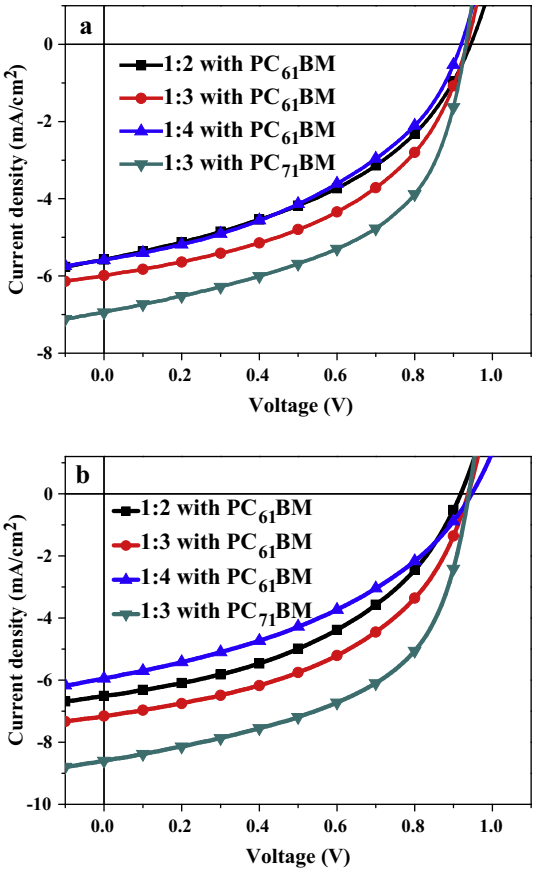

Fig. 5. *J–V* curves of the BHJ OSCs based on DCAO3TIDT (a) and DCNR3TIDT (b) as donor and $PC_{61}BM$ or $PC_{71}BM$ as acceptor with different weight ratio (1:2–1:4).

(600 MHz, $CDCl_3$) δ 8.24 (s, 2H), 7.66 (d, J = 4.1 Hz, 2H), 7.36 (s, 2H), 7.31 (d, J = 3.8 Hz, 2H), 7.22 (d, J = 4.0 Hz, 2H), 7.19 (d, J = 8.8 Hz, 8H), 7.11 (dd, J = 5.0, 4.1 Hz, 4H), 7.08 (d, J = 5.1 Hz, 4H), 6.80 (d, J = 8.8 Hz, 8H), 4.25–4.19 (m, 4H), 3.91 (t, J = 6.5 Hz, 8H), 1.78–1.69 (m, 10H), 1.45–1.24 (m, 88H), 0.96–0.90 (m, 12H), 0.87 (t, J = 7.0 Hz, 12H). ^{13}C NMR (150 MHz, $CDCl_3$) δ 163.15, 162.10, 158.18, 157.65, 157.09, 156.82, 153.80, 150.68, 146.99, 146.55, 145.95, 145.57, 140.46, 139.31, 139.22, 139.11, 138.74, 138.23, 138.15, 136.13, 135.50, 135.02, 134.72, 134.29, 134.20, 132.51, 129.02, 127.39, 125.29, 124.65, 124.25, 124.00, 119.73, 117.10, 115.95, 114.32, 97.77, 68.82, 67.97, 62.32, 38.80, 31.91, 30.32, 29.66, 29.63, 29.60, 29.58, 29.41, 29.34, 29.31, 28.93, 26.09, 23.77, 22.95, 22.69, 14.12, 14.05, 11.02. Anal. Calc. for $C_{136}H_{168}N_2O_8S_8$: C, 73.73; H, 7.64; N, 1.26; S, 11.58. Found: C, 73.64; H, 7.56; N, 1.30; S, 11.50.

Synthesis of DCNR3TIDT

A solution of DCHO3TIDT (0.2 g, 0.1 mmol), 2-(1,1-dicyanomethylene)-3-octyl rhodanine (0.2 g, 0.7 mmol), CH_3COONH_4 (0.5 g, 6.5 mmol), and chlorobenzene (15 mL) in CH_3COOH (30 mL) was degassed with argon. Then the mixture was refluxed for 48 h. After the reaction was completed, the mixture was poured into water and extracted with CH_2Cl_2. The organic layer was washed with water and dried over Na_2SO_4. After removal of solvent, the crude product was purified with column chromatography on silica gel using a mixture of CH_2Cl_2 and petroleum ether (2:1) as eluant to afford compound DCNR3TIDT (43.5 mg, 17%) as a black solid. ^1H NMR (600 MHz, $CDCl_3$) δ 8.02 (s, 2H), 7.39 (d, J = 4.0 Hz, 2H), 7.36 (s, 2H), 7.30 (d, J = 3.8 Hz, 2H), 7.24 (d, J = 3.9 Hz, 2H), 7.19 (d, J = 8.8 Hz, 8H), 7.12 (t, J = 4.0 Hz, 4H), 7.08 (d, J = 5.4 Hz, 4H), 6.80 (d, J = 8.8 Hz, 8H), 4.23–4.18 (m, 4H), 3.91 (t, J = 6.5 Hz, 8H), 1.77–1.72 (m, 12H), 1.42–1.24 (m, 92H), 0.87 (m, 18H). ^{13}C NMR (150 MHz, $CDCl_3$) δ 165.99, 165.43, 158.17, 157.09, 153.79, 146.10, 140.47, 139.30, 139.01, 138.23, 136.63, 136.13, 135.21, 135.02, 134.69, 134.06, 129.02, 128.54, 127.04, 125.26, 124.96, 124.63, 123.99, 119.73, 117.10, 114.31, 113.49, 113.32, 112.27, 67.97, 62.32, 55.86, 45.38, 31.91, 31.71, 29.66, 29.63, 29.60, 29.58, 29.41, 29.34, 29.31, 29.09, 29.05, 28.82, 26.09, 25.96, 22.69, 22.61, 14.13, 14.08. Anal. Calc. for $C_{142}H_{168}N_6O_6S_{10}$: C, 71.80; H, 7.13; N, 3.54; S, 13.50. Found: C, 71.72; H, 7.21; N, 3.59; S, 13.41.

3. Results and discussion

3.1. Optical properties

Fig. 1 shows the UV–vis absorption spectra of DCAO3TIDT and DCNR3TIDT in dilute $CHCl_3$ solutions and in the solid films on quartz plate, and the parameters are summarized in Table 1. Compared with the absorption spectra in the solutions, the absorption peaks of DCAO3TIDT and DCNR3TIDT in the solid films are red shifted about 9 nm and 15 nm, respectively, which may be caused by the molecular aggregates. In addition, it is noted that DCNR3TIDT exhibits a more broad absorption with two peaks compared to DCAO3TIDT. It is believed to be induced mainly by strong electron withdrawing rhodanine and malononitrile groups on CNR. Obviously, the electron withdrawing ability of CNR is stronger than CAO unit. On the

Table 2
OSCs performance of DCAO3TIDT and DCNR3TIDT as donor materials.

Active layer	Weight ratio	V_{oc} (V)	J_{sc} (mA/cm^2)	FF (%)	PCE_{max} (PCE_{ave}) (%)
DCAO3TIDT:$PC_{61}BM$	1:2	0.94	5.57	42.85	2.25 (2.06)
	1:3	0.93	5.99	47.17	2.63 (2.35)
	1:4	0.91	5.58	42.32	2.17 (2.02)
	1:3[a]	0.92	5.47	41.46	2.09 (1.96)
DCAO3TIDT:$PC_{71}BM$	1:3	0.93	6.93	51.71	3.34 (3.14)
DCNR3TIDT:$PC_{61}BM$	1:2	0.92	6.51	44.06	2.63 (2.41)
	1:3	0.94	7.16	47.14	3.16 (2.97)
	1:4	0.94	5.94	39.90	2.24 (2.03)
	1:3[a]	0.91	6.36	42.00	2.42 (2.28)
DCNR3TIDT:$PC_{71}BM$	1:3	0.94	8.59	52.95	4.27 (4.12)

[a] 80 °C annealing 10 min.

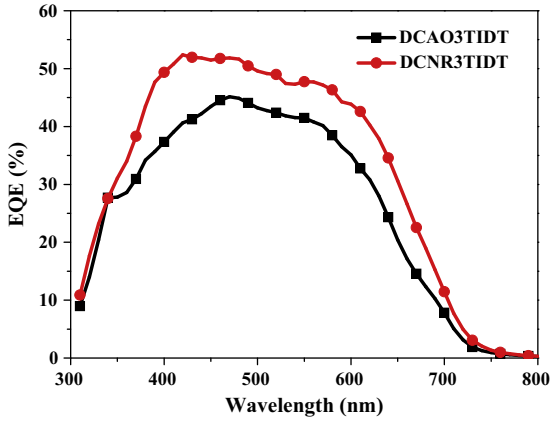

Fig. 6. EQE curves of the BHJ OSCs based on DCAO3TIDT/$PC_{71}BM$ (1:3, w/w) and DCNR3TIDT/$PC_{71}BM$ (1:3, w/w).

other hand, the nitrogen and sulfur atoms in the CNR ring have lone electron pairs, which increase the conjugated units to lead to broad absorption [26,40]. The optical band gaps of DCAO3TIDT and DCNR3TIDT thin films were estimated from the onsets of the film absorption spectra to be 1.87 eV and 1.73 eV.

3.2. Thermal properties

Thermal stability of the two molecules was investigated with TGA under a nitrogen atmosphere, and the results are shown in Fig. 2. It reveals that the onset temperature with 5% weight-loss (T_d) of DCAO3TIDT and DCNR3TIDT is 386 °C, and 400 °C, respectively. Obviously, the thermal stability of the two molecules is adequate for the application in OSCs and other optoelectronic devices.

3.3. Electrochemical properties

Cyclic voltammetry (CV) has been widely employed to investigate the electrochemical behavior of the molecules and estimate their HOMO and LUMO energy levels [41,42]. As shown in Fig. 3, only oxidation potentials were recorded for the two molecules. The HOMO energy levels of the molecules can be calculated from their onset oxidation potentials (φ_{ox}) according to the equation: $E_{HOMO} = -e(\varphi_{ox} + 4.8 - \varphi_{1/2,\ FeCp2})$ (eV), where the unit of potential is V vs. Hg/Hg_2Cl_2. The LUMO was derived from HOMO and E_g^{opt}, LUMO = HOMO + E_g^{opt}. Thus the HOMO and LUMO energy levels of DCAO3TIDT are −5.29 eV and −3.42 eV, and the values for DCNR3TIDT are −5.33 eV and −3.60 eV (Table 1). The relatively low HOMO energy levels of the two molecules are beneficial to obtain high V_{oc} for OSCs with them as donor materials.

3.4. Hole mobility

The hole mobilities of DCAO3TIDT and DCNR3TIDT were measured employing the vertical diodes with structure of ITO/PEDOT:PSS/DCAO3TIDT (or DCNR3TIDT)/Au according to the space-charge-limited-current model [43]. The mobilities are about 2.5×10^{-5} cm^2/V s and 1.4×10^{-5} cm^2/V s for DCAO3TIDT and DCNR3TIDT, respectively. The corresponding current density–voltage curves are given in Fig. 4.

3.5. Photovoltaic properties

BHJ OSCs were fabricated by using DCAO3TIDT and DCNR3TIDT as the donor materials, and $PC_{61}BM$ or $PC_{71}BM$ as the acceptor, using the conventional solution spin-coating process. The device structure is ITO/PEDOT:PSS/active layer/Ca/Al. The *J–V* curves of the BHJ OSCs were shown in Fig. 5 and the results were summarized in Table 2. For DCAO3TIDT, the optimal efficiency was obtained from the device with the active layer comprised of a blend of DCAO3TIDT and $PC_{71}BM$ with a weight ratio of 1:3. This BHJ OSCs shows a V_{oc} of 0.93 V, a J_{sc} of 6.93 mA/cm^2, a FF of 51.71% and a PCE of 3.34%. By comparison, the optimal BHJ OSCs device based on DCNR3TIDT:$PC_{71}BM$ (1:3, w/w) blend showed a V_{oc} of 0.94 V, a J_{sc} of 8.59 mA/cm^2, a FF of 52.95% and a PCE of 4.27%. From Fig. 5 and Table 2, it can be seen that all the devices exhibited typical characteristics with high V_{oc} ($\geqslant$0.91 V), and they were insensitive to the donor/acceptor weight ratio. The high V_{oc} is ascribed to the deep HOMO energy levels of the two molecules.

Fig. 6 shows the EQE curves of the small molecules BHJ OSCs based on DCAO3TIDT/$PC_{71}BM$ (1:3, w/w) and DCNR3TIDT/$PC_{71}BM$ (1:3, w/w) under the optimized fabrication condition. It can be seen that the device based

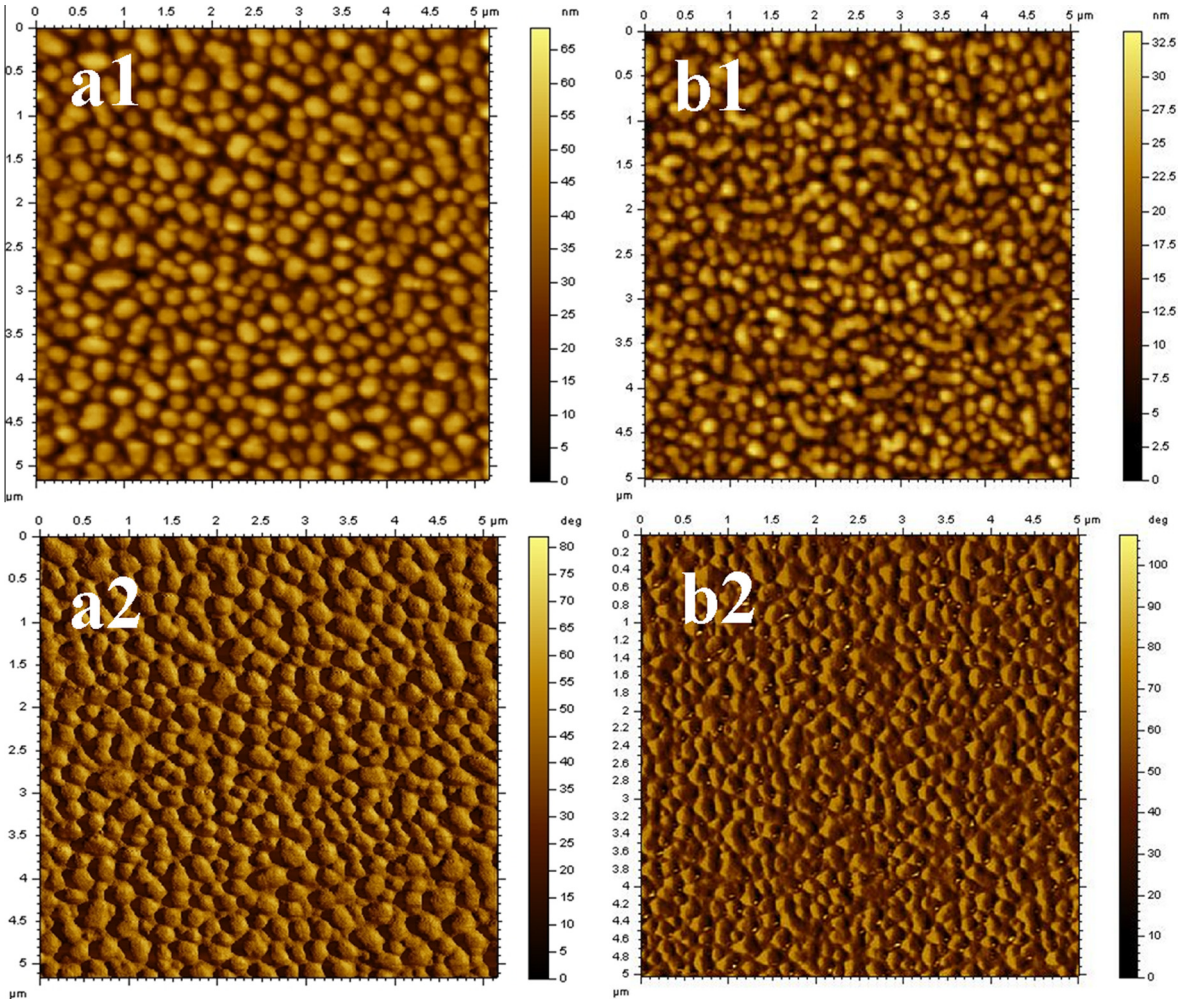

Fig. 7. AFM images: (top) topography images, (bottom) phase images of the blend films of DCAO3TIDT/$PC_{71}BM$ (1:3, w/w) (a1, a2) and DCNR3TIDT/$PC_{71}BM$ (1:3, w/w) (b1, b2), the scan size of the images is 5 μm × 5 μm.

on DCNR3TIDT shows wider and higher EQE curve than the device based on DCAO3TIDT, which is consistent with their absorption spectra (Fig. 1). The J_{sc} of devices based on DCAO3TIDT and DCNR3TIDT calculated from the EQE curves are 6.87 mA/cm^2 and 8.52 mA/cm^2, respectively, which are well in accord with the J_{sc} recorded from *J–V* curves (Table 2). In view of the two molecules having the same chemical core structure, it was presumed that the higher J_{sc} for DCNR3TIDT was ascribed to the end-capped block CNR, which shows stronger electron withdrawing ability than CAO unit, resulted in broader absorption. Finally, the device based on DCNR3TIDT exhibits a higher PCE than DCAO3TIDT-based device.

The nanoscale phase separation of the active layer is preferable morphology to obtain high performance OSCs, which enables a large interface area for exciton dissociation and, in the mean time, a continuous percolating path for hole and electron transport to the corresponding electrodes [44–47]. In order to clarify the difference in performance of the two BHJ OSCs, the morphologies of the two active layers were investigated by AFM technique in tapping mode. Fig. 7 shows the AFM topographic and phase images of the blend films of DCAO3TIDT/$PC_{71}BM$ (1:3, w/w) and DCNR3TIDT/$PC_{71}BM$ (1:3, w/w). The root-mean-square (RMS) roughness of DCAO3TIDT and DCNR3TIDT are about 11.5 nm and 5.44 nm, respectively. Apparently, the blend film of DCAO3TIDT/$PC_{71}BM$ is typical cluster structures with larger aggregated domains and higher roughness than the film of DCNR3TIDT/$PC_{71}BM$. The large phase separation scale is unfavorable for exciton diffusion [48], which is another important factor for the lower J_{sc} of the device based on DCAO3TIDT/$PC_{71}BM$. Consequently, the PCE of the device deceased to 3.34%, lower than the DCNR3TIDT:$PC_{71}BM$ system.

4. Conclusion

Two electron withdrawing end-capped blocks CAO and CNR were introduced into the IDT backbone, formulating two A–D–A type small molecules DCAO3TIDT and DCNR3TIDT. Both of them showed deep HOMO energy levels and high thermal stability. The BHJ OSCs based on

DCAO3TIDT/$PC_{71}BM$ and DCNR3TIDT/$PC_{71}BM$ showed high V_{oc} (~0.93 V), and PCE of 3.34% and 4.27%, respectively, under the illumination of AM 1.5 G, 100 mW/cm^2. The relatively higher photovoltaic performance of DCNR3TIDT/$PC_{71}BM$ was ascribed to the end-capped moiety, bearing in mind that the two molecules have same chemical core structure. The results indicated that CNR moiety as a strong electron withdrawing end-capped block in A–D–A type small molecules can significantly extend absorption spectra as expected, resulting in a relatively high J_{sc}, and meanwhile still remain high V_{oc}.

Acknowledgements

This work was supported by the Ministry of Science and Technology of China (2014CB643501 and 2010DFA52310), the National Natural Science Foundation of China (51173199, 51211140346 and 61405209), Shandong Provincial Natural Science Foundation (ZR2011BZ007), and Qingdao Municipal Science and Technology Program (11-2-4-22-hz).

References

[1] G. Yu, J. Gao, J.C. Hummelen, F. Wudl, A.J. Heeger, Polymer photovoltaic cells – enhanced efficiencies via a network of internal donor–acceptor heterojunctions, Science 270 (1995) 1789–1791.
[2] L. Dou, C.-C. Chen, K. Yoshimura, K. Ohya, W.-H. Chang, J. Gao, Y. Liu, E. Richard, Y. Yang, Synthesis of 5H-dithieno[3,2-b:2′,3′-d]pyran as an electron-rich building block for donor–acceptor type low-bandgap polymers, Macromolecules 46 (2013) 3384–3390.
[3] Y. Huang, M. Zhang, H. Chen, F. Wu, Z. Cao, L. Zhang, S. Tan, Efficient polymer solar cells based on terpolymers with a broad absorption range of 300–900 nm, J. Mater. Chem. A 2 (2014) 5218.
[4] I. Osaka, T. Kakara, N. Takemura, T. Koganezawa, K. Takimiya, Naphthodithiophene–naphthobisthiadiazole copolymers for solar cells: alkylation drives the polymer backbone flat and promotes efficiency, J. Am. Chem. Soc. 135 (2013) 8834–8837.
[5] S. Liu, K. Zhang, J. Lu, J. Zhang, H.L. Yip, F. Huang, Y. Cao, High-efficiency polymer solar cells via the incorporation of an amino-functionalized conjugated metallopolymer as a cathode interlayer, J. Am. Chem. Soc. 135 (2013) 15326–15329.
[6] J. Hou, Z. Tan, Y. Yan, Y. He, C. Yang, Y. Li, Synthesis and photovoltaic properties of two-dimensional conjugated polythiophenes with bi(thienylenevinylene) side chains, J. Am. Chem. Soc. 128 (2006) 4911–4916.
[7] C. Cabanetos, A. El Labban, J.A. Bartelt, J.D. Douglas, W.R. Mateker, J.M. Frechet, M.D. McGehee, P.M. Beaujuge, Linear side chains in benzo[1,2-b:4,5-b′]dithiophene–thieno[3,4-c]pyrrole-4, 6-dione polymers direct self-assembly and solar cell performance, J. Am. Chem. Soc. 135 (2013) 4656–4659.
[8] T.B. Yang, M. Wang, C.H. Duan, X.W. Hu, L. Huang, J.B. Peng, F. Huang, X. Gong, Inverted polymer solar cells with 8.4% efficiency by conjugated polyelectrolyte, Energy Environ. Sci. 5 (2012) 8208–8214.
[9] H.C. Chen, Y.H. Chen, C.C. Liu, Y.C. Chien, S.W. Chou, P.T. Chou, Prominent short-circuit currents of fluorinated quinoxaline-based copolymer solar cells with a power conversion efficiency of 8.0%, Chem. Mater. 24 (2012) 4766–4772.
[10] K.H. Hendriks, G.H. Heintges, V.S. Gevaerts, M.M. Wienk, R.A. Janssen, High-molecular-weight regular alternating diketopyrrolopyrrole-based terpolymers for efficient organic solar cells, Angew. Chem. 52 (2013) 8341–8344.
[11] F.S. Kim, X. Guo, M.D. Watson, S.A. Jenekhe, High-mobility ambipolar transistors and high-gain inverters from a donor–acceptor copolymer semiconductor, Adv. Mater. 22 (2010) 478–482.
[12] Z. He, C. Zhong, X. Huang, W.Y. Wong, H. Wu, L. Chen, S. Su, Y. Cao, Simultaneous enhancement of open-circuit voltage, short-circuit current density, and fill factor in polymer solar cells, Adv. Mater. 23 (2011) 4636–4643.
[13] D. Ma, M. Lv, M. Lei, J. Zhu, H. Wang, X. Chen, Self-organization of amine-based cathode interfacial materials in inverted polymer solar cells, ACS Nano 8 (2014) 1601–1608.
[14] M. Lv, M. Lei, J. Zhu, T. Hirai, X. Chen, [6,6]-Phenyl-C61-butyric Acid 2-((2-(dimethylamino)ethyl)(methyl)amino)-ethyl ester as an acceptor and cathode interfacial material in polymer solar cells, ACS Appl. Mater. Interfaces 6 (2014) 5844–5851.
[15] X. Guo, M. Baumgarten, K. Müllen, Designing π-conjugated polymers for organic electronics, Prog. Polym. Sci. 38 (2013) 1832–1908.
[16] T. Qin, W. Zajaczkowski, W. Pisula, M. Baumgarten, M. Chen, M. Gao, G. Wilson, C.D. Easton, K. Mullen, S.E. Watkins, Tailored donor–acceptor polymers with an a–d1–a–d2 structure: controlling intermolecular interactions to enable enhanced polymer photovoltaic devices, J. Am. Chem. Soc. 136 (2014) 6049–6055.
[17] Y. Sun, G.C. Welch, W.L. Leong, C.J. Takacs, G.C. Bazan, A. Heeger, Solution-processed small-molecule solar cells with 6.7% efficiency, Nat. Mater. 11 (2012) 44–48.
[18] G.C. Welch, L.A. Perez, C.V. Hoven, Y. Zhang, X.D. Dang, A. Sharenko, M.F. Toney, E.J. Kramer, T.Q. Nguyen, G.C. Bazan, A modular molecular framework for utility in small-molecule solution-processed organic photovoltaic devices, J. Mater. Chem. 21 (2011) 12700–12709.
[19] J.Y. Zhou, X.J. Wan, Y.S. Liu, G.K. Long, F. Wang, Z. Li, Y. Zuo, C.X. Li, Y.S. Chen, A Planar small molecule with dithienosilole core for high efficiency solution-processed organic photovoltaic cells, Chem. Mater. 23 (2011) 4666–4668.
[20] D. Demeter, T. Rousseau, P. Leriche, T. Cauchy, R. Po, J. Roncali, Manipulation of the open-circuit voltage of organic solar cells by desymmetrization of the structure of acceptor–donor–acceptor molecules, Adv. Funct. Mater. 21 (2011) 4379–4387.
[21] A. Salleo, R.J. Kline, D.M. DeLongchamp, M.L. Chabinyc, Microstructural characterization and charge transport in thin films of conjugated polymers, Adv. Mater. 22 (2010) 3812–3838.
[22] J. Zhou, Y. Zuo, X. Wan, G. Long, Q. Zhang, W. Ni, Y. Liu, Z. Li, G. He, C. Li, B. Kan, M. Li, Y. Chen, Solution-processed and high-performance organic solar cells using small molecules with a benzodithiophene unit, J. Am. Chem. Soc. 135 (2013) 8484–8487.
[23] J.L. Bredas, J.R. Durrant, Organic photovoltaics, Acc. Chem. Res. 42 (2009) 1689–1690.
[24] L. Ye, S. Zhang, L. Huo, M. Zhang, J. Hou, Molecular design toward highly efficient photovoltaic polymers based on two-dimensional conjugated benzodithiophene, Acc. Chem. Res. 47 (2014) 1595–1603.
[25] Y. Li, Molecular design of photovoltaic materials for polymer solar cells: toward suitable electronic energy levels and broad absorption, Acc. Chem. Res. 45 (2012) 723–733.
[26] A. Insuasty, A. Ortiz, A. Tigreros, E. Solarte, B. Insuasty, N. Martin, 2-(1,1-Dicyanomethylene)rhodanine A novel, efficient electron acceptor, Dyes Pigm. 88 (2011) 385–390.
[27] V. Pushkara Rao, A.K.-Y. Jen, J.B. Caldwell, Rhodanine-methine as π-electron acceptor in second-order nonlinear optical chromophores, Tetrahedron Lett. 35 (1994) 3849–3852.
[28] J. Ray, N. Panja, P.K. Nandi, J.J. Martin, W.E. Jones, Spectroscopic and ab initio study of an intramolecular charge transfer (ICT) rhodanine derivative, J. Mol. Struct. 874 (2008) 121–127.
[29] G. He, Z. Li, X. Wan, Y. Liu, J. Zhou, G. Long, M. Zhang, Y. Chen, Impact of dye end groups on acceptor–donor–acceptor type molecules for solution-processed photovoltaic cells, J. Mater. Chem. 22 (2012) 9173.
[30] J. Mao, N. He, Z. Ning, Q. Zhang, F. Guo, L. Chen, W. Wu, J. Hua, H. Tian, Stable dyes containing double acceptors without COOH as anchors for highly efficient dye-sensitized solar cells, Angew. Chem. 51 (2012) 9873–9876.
[31] Y. Lin, Z.G. Zhang, H. Bai, Y. Li, X. Zhan, A star-shaped oligothiophene end-capped with alkyl cyanoacetate groups for solution-processed organic solar cells, Chem. Commun. 48 (2012) 9655–9657.
[32] K. Wang, Y. Zhao, W. Tang, Z.-G. Zhang, Q. Fu, Y. Li, High open-circuit voltage polymer solar cells based on D–A copolymer of indacenodithiophene and fluorine-substituted benzotriazole, Org. Electron. 15 (2014) 818–823.
[33] Y. Zhang, J.Y. Zou, H.L. Yip, K.S. Chen, J.A. Davies, Y. Sun, A.K.Y. Jen, Synthesis, characterization, charge transport, and photovoltaic properties of dithienobenzoquinoxaline- and dithienobenzopyridopyrazine-based conjugated polymers, Macromolecules 44 (2011) 4752–4758.
[34] M. Zhang, X. Guo, X. Wang, H. Wang, Y. Li, Synthesis and photovoltaic properties of D–A copolymers based on alkyl-substituted indacenodithiophene donor unit, Chem. Mater. 23 (2011) 4264–4270.

[35] Y.C. Chen, C.Y. Yu, Y.L. Fan, L.I. Hung, C.P. Chen, C. Ting, Low-bandgap conjugated polymer for high efficient photovoltaic applications, Chem. Commun. 46 (2010) 6503–6505.
[36] X. Guo, M. Zhang, J. Tan, S. Zhang, L. Huo, W. Hu, Y. Li, J. Hou, Influence of D/A ratio on photovoltaic performance of a highly efficient polymer solar cell system, Adv. Mater. 24 (2012) 6536–6541.
[37] J.L.G. Ruano, J. Aleman, I. Alonso, A. Parra, V. Marcos, J. Aguirre, Pi–pi stacking vs. steric effects in stereoselectivity control: highly diastereoselective synthesis of syn-1,2-diarylpropylamines, Chemistry 13 (2007) 6179–6195.
[38] M.H. Chen, J. Hou, Z. Hong, G. Yang, S. Sista, L.M. Chen, Y. Yang, Efficient polymer solar cells with thin active layers based on alternating polyfluorene copolymer/fullerene bulk heterojunctions, Adv. Mater. 21 (2009) 4238–4242.
[39] S. Higashijima, H. Miura, T. Fujita, Y. Kubota, K. Funabiki, T. Yoshida, M. Matsui, Highly efficient new indoline dye having strong electron-withdrawing group for zinc oxide dye-sensitized solar cell, Tetrahedron 67 (2011) 6289–6293.
[40] T. Horiuchi, H. Miura, K. Sumioka, S. Uchida, High efficiency of dye-sensitized solar cells based on metal-free indoline dyes, J. Am. Chem. Soc. 126 (2004) 12218–12219.
[41] J.C. Bijleveld, A.P. Zoombelt, S.G. Mathijssen, M.M. Wienk, M. Turbiez, D.M. de Leeuw, R.A. Janssen, Poly(diketopyrrolopyrrole–terthiophene) for ambipolar logic and photovoltaics, J. Am. Chem. Soc. 131 (2009) 16616–16617.
[42] L. Dou, W.H. Chang, J. Gao, C.C. Chen, J. You, Y. Yang, A selenium-substituted low-bandgap polymer with versatile photovoltaic applications, Adv. Mater. 25 (2013) 825–831.
[43] V.D. Mihailetchi, J. Wildeman, P.W. Blom, Space-charge limited photocurrent, Phys. Rev. Lett. 94 (2005) 126602.
[44] Q. Zheng, B.J. Jung, J. Sun, H.E. Katz, Ladder-type oligo-p-phenylene-containing copolymers with high open-circuit voltages and ambient photovoltaic activity, J. Am. Chem. Soc. 132 (2010) 5394–5404.
[45] X.C. Bao, T. Wang, A.L. Yang, C.P. Yang, X.W. Dou, W.C. Chen, N. Wang, R.Q. Yang, Annealing-free P3HT:PCBM-based organic solar cells via two halohydrocarbons additives with similar boiling points, Mater. Sci. Eng. B – Adv. 180 (2014) 7–11.
[46] T.J. Savenije, J.E. Kroeze, X.N. Yang, J. Loos, The effect of thermal treatment on the morphology and charge carrier dynamics in a polythiophene–fullerene bulk heterojunction, Adv. Funct. Mater. 15 (2005) 1260–1266.
[47] L.L. Chang, H.W.A. Lademann, J.B. Bonekamp, K. Meerholz, A.J. Moule, Effect of trace solvent on the morphology of P3HT:PCBM bulk heterojunction solar cells, Adv. Funct. Mater. 21 (2011) 1779–1787.
[48] C.J. Brabec, N.S. Sariciftci, J.C. Hummelen, Plastic solar cells, Adv. Funct. Mater. 11 (2001) 15–26.